

Multi-differential measurement of the dijet cross section in proton-proton collisions at $\sqrt{s} = 13 \text{ TeV}$ with CMS

PhD student
Polidamas Georgios Kosmoglou Kioseoglou
University of Ioannina

HEP 2023 - 40th Conference on Recent Developments in High Energy Physics and Cosmology, Ioannina, Greece

Friday, 7th April 2023



- **Introduction**

- Motivation
- Observables

- Unfolding

- Theory

- QCD analysis

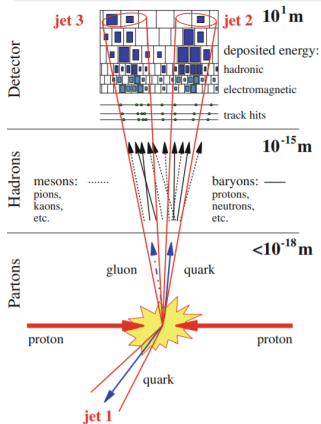
- Summary

- Back Up



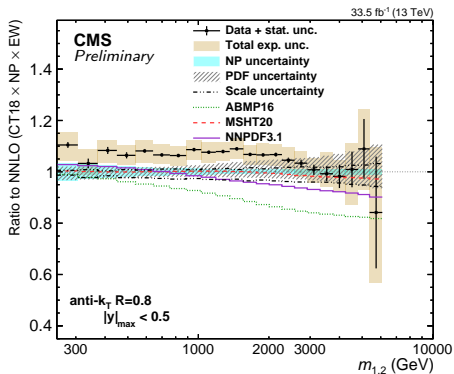
Introduction – Motivation

- 1 Precise jet measurements.
- 2 Comparison to NNLO pQCD predictions.
- 3 Improve Parton Distribution Functions.
- 4 Extract strong coupling constant α_S .



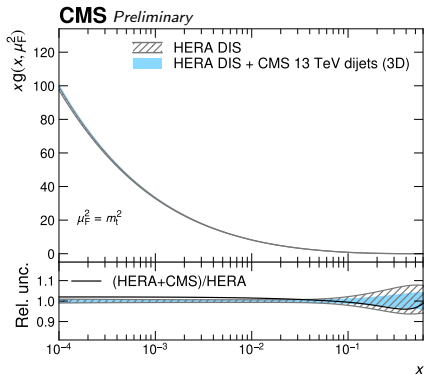
Introduction – Motivation

- 1 Precise jet measurements.
- 2 Comparison to NNLO pQCD predictions.
- 3 Improve Parton Distribution Functions.
- 4 Extract strong coupling constant α_s .



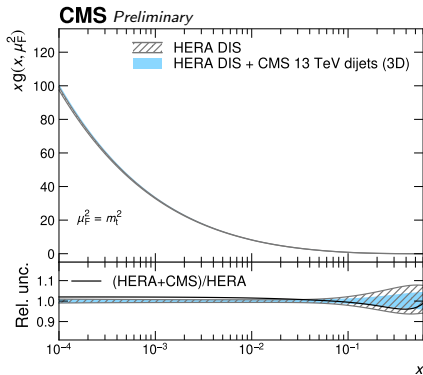
Introduction – Motivation

- 1 Precise jet measurements.
- 2 Comparison to NNLO pQCD predictions.
- 3 Improve Parton Distribution Functions.
- 4 Extract strong coupling constant α_S .



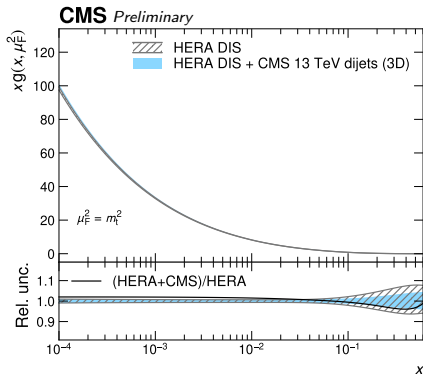
Introduction – Motivation

- 1 Precise jet measurements.
- 2 Comparison to NNLO pQCD predictions.
- 3 Improve Parton Distribution Functions.
- 4 Extract strong coupling constant α_S .



Introduction – Motivation

- 1 Precise jet measurements.
- 2 Comparison to NNLO pQCD predictions.
- 3 Improve Parton Distribution Functions.
- 4 Extract strong coupling constant α_S .



Physics Analysis Summary (PAS)

All results shown in this presentation are contained within [SMP-21-008](#)

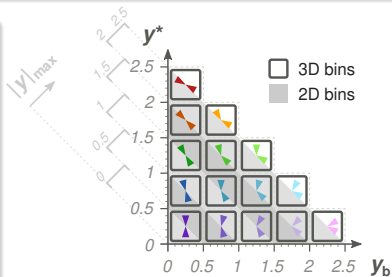


Six dijet measurements

- 2016 data of $\mathcal{L}_{int} = 36.3 \text{ fb}^{-1}$ at 13 TeV.
- Jet reconstruction via **anti- k_T** (PFchsJets).
- One entry per event.
- Requiring at least **two jets** for either

$$\langle p_T \rangle_{1,2} = \frac{1}{2}(p_{T,1} + p_{T,2}),$$

$$\text{or } m_{1,2} = \sqrt{(E_1 + E_2)^2 - (\vec{p}_1 + \vec{p}_2)^2}.$$

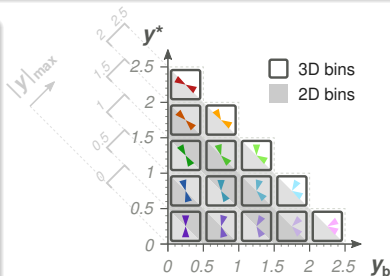


Six dijet measurements

- 2016 data of $\mathcal{L}_{int} = 36.3 \text{ fb}^{-1}$ at 13 TeV.
- Jet reconstruction via **anti- k_T** (PFchsJets).
- One entry per event.
- Requiring at least **two jets** for either

$$\langle p_T \rangle_{1,2} = \frac{1}{2}(p_{T,1} + p_{T,2}),$$

$$\text{or } m_{1,2} = \sqrt{(E_1 + E_2)^2 - (\vec{p}_1 + \vec{p}_2)^2}.$$



#2 – Double-differential (2D)

$$\bullet \frac{d^2\sigma}{dy_{max} dm_{1,2}} = \frac{1}{\epsilon \mathcal{L}_{int}} \frac{N}{(2\Delta|y|_{max})\Delta m_{1,2}},$$

$$|y|_{max} = \max(|y_1|, |y_2|).$$

- Jet size $R = 0.4$ and $R = 0.8$.
- Phase space:

$$p_{T,1} \geq 100 \text{ GeV} \quad , \quad p_{T,2} \geq 50 \text{ GeV}$$

$$|y_1| < 2.5 \quad , \quad |y_2| < 2.5$$

#4 – Triple-differential (3D)

$$\bullet \frac{d^3\sigma}{dy^* dy_b dx} = \frac{1}{\epsilon \mathcal{L}_{int}} \frac{N}{\Delta y^* \Delta y_b \Delta x},$$

$$y^* = 1/2|y_1 - y_2|, \quad y_b = 1/2|y_1 + y_2|$$

and $x = m_{1,2}$ or $\langle p_T \rangle_{1,2}$.

- Jet size $R = 0.4$ and $R = 0.8$.
- Phase space:

$$p_{T,1} \geq 100 \text{ GeV} \quad , \quad p_{T,2} \geq 50 \text{ GeV}$$

$$|y_1| < 3.0 \quad , \quad |y_2| < 3.0$$



- Introduction
- **Unfolding**
- Theory
- QCD analysis
- Summary
- Back Up



Unfolding – Probability matrix

The task

Particle level distributions \leftarrow Detector level distributions

Solution: Least-square minimization

$$\chi^2 = (y - Ax - b)^T (V_y)^{-1} (y - Ax - b)$$

- Multi-D unfolding (TUnfold) :
 - * Background (fakes)
 - * Unsmear
 - * Inefficiencies (misses)
- Probability matrix constructed by Pythia 8.
- Condition Number $\sim 3 < 10$.



Unfolding – Probability matrix

The task

Particle level distributions \leftarrow Detector level distributions

Solution: Least-square minimization

$$\chi^2 = (y - Ax - b)^T (V_y)^{-1} (y - Ax - b)$$

- Multi-D unfolding (TUnfold) :
 - * Background (fakes)
 - * Unsmear
 - * Inefficiencies (misses)
- Probability matrix constructed by Pythia 8.
- Condition Number $\sim 3 < 10$.



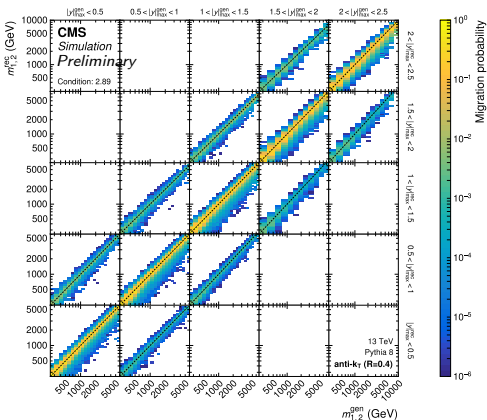
Unfolding – Probability matrix

The task

Particle level distributions ← Detector level distributions

Solution: Least-square minimization

$$\chi^2 = (y - Ax - b)^T (V_y)^{-1} (y - Ax - b)$$



- Multi-D unfolding (TUnfold) :
 - * Background (fakes)
 - * Unsmear
 - * Inefficiencies (misses)
- Probability matrix constructed by Pythia 8.
- Condition Number $\sim 3 < 10$.

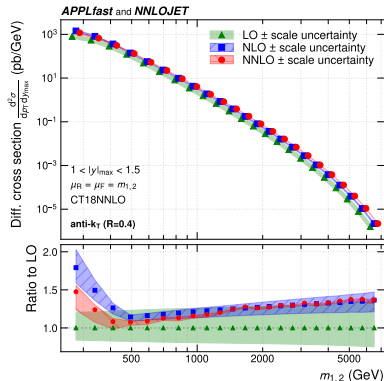


- Introduction
- Unfolding
- **Theory**
 - Fixed order predictions
 - Data comparison
- QCD analysis
- Summary
- Back Up



Predictions at NNLO pQCD:

- Obtained with the NNLOJET program as FASTNLO interpolation tables with the APPLFAST interface^[1].
- $\mu_R = \mu_F = m_{1,2}$.
- Combined with the **CT18 @ NNLO** PDF set.



[1]: D. Britzger et al., "NNLO interpolation grids for jet production at the LHC", *Eur. Phys. J.C* **82** (2022) 930,

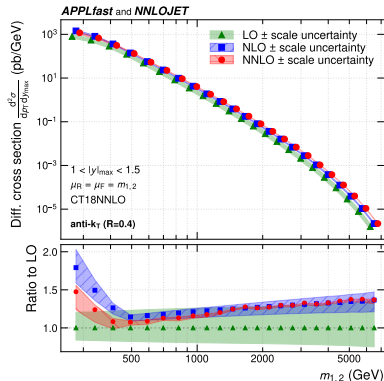
[doi:10.1140/epjc/s10052-022-10880-2](https://doi.org/10.1140/epjc/s10052-022-10880-2), [arXiv:2207.13735](https://arxiv.org/abs/2207.13735).



Predictions at NNLO pQCD:

- Obtained with the NNLOJET program as FASTNLO interpolation tables with the APPLFAST interface^[1].
- $\mu_R = \mu_F = m_{1,2}$.
- Combined with the **CT18 @ NNLO** PDF set.

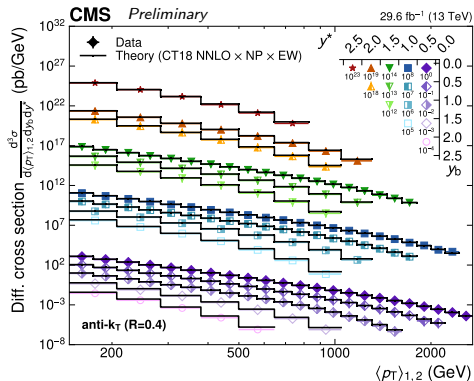
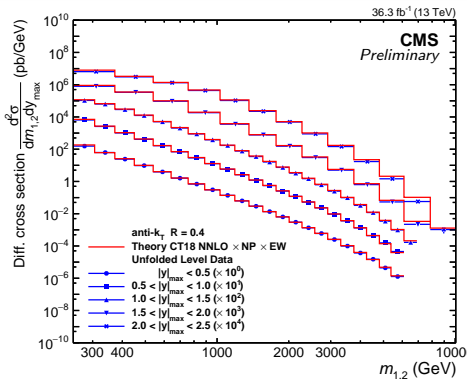
- Scale uncertainty is **reduced** for higher orders.
- Higher order corrections mostly within scale uncertainty band of lower orders.



[1]: D. Britzger et al., “NNLO interpolation grids for jet production at the LHC”, *Eur. Phys. J.C* **82** (2022) 930,

[doi:10.1140/epjc/s10052-022-10880-2](https://doi.org/10.1140/epjc/s10052-022-10880-2), [arXiv:2207.13735](https://arxiv.org/abs/2207.13735).

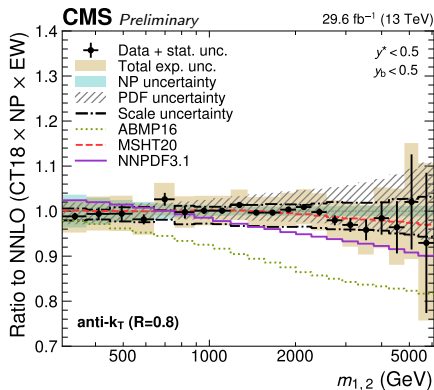
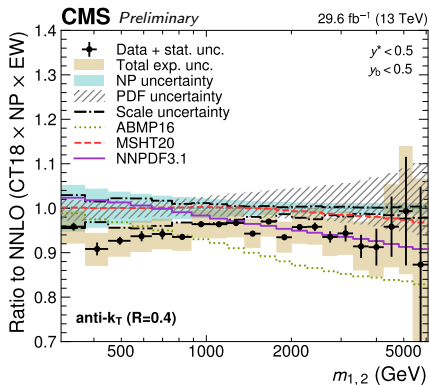
Theory – Data comparison



- Fixed order predictions at NNLO corrected for **NP** (Non-Perturbative) and **EW** (ElectroWeak) effects (details in [backup](#)).
- Steeply falling distributions.
- Data and Theory seem to be compatible across all observable bins.



Theory – Data comparison



- Good agreement in most phase space regions, mostly **below 10%** (details in [backup](#)).
- Better description for $R = 0.8$ measurements compared to $R = 0.4$.
- Additional comparisons between other PDFs are performed. Best agreement to CT18 (default) is displayed by **MSHT20**.



- Introduction
- Unfolding
- Theory
- **QCD analysis**
- Summary
- Back Up



QCD analysis performed with both 2D and 3D cross sections:

- as a function of $\mathbf{m}_{1,2}$ to reach the higher end of the phase space.
(*indications of a smaller impact to subleading color corrections compared to $\langle p_T \rangle_{1,2}$.)
- using wider jet cone size $\mathbf{R} = 0.8$ to profit from increased agreement displayed by NNLO pQCD predictions.

[1]: H1 and ZEUS Collaborations, “Combination of measurements of inclusive deep inelastic $e\pm p$ scattering cross sections and QCD analysis of HERA data”, *Eur. Phys. J. C* **75** (2015) 580, [doi:10.1140/epjc/s10052-015-3710-4](https://doi.org/10.1140/epjc/s10052-015-3710-4), [arXiv:1506.06042](https://arxiv.org/abs/1506.06042).



QCD analysis – Fit details | *PDF-only* fits

QCD analysis performed with both **2D** and **3D** cross sections:

- as a function of $\mathbf{m}_{1,2}$ to reach the higher end of the phase space.
(*indications of a smaller impact to subleading color corrections compared to $\langle p_T \rangle_{1,2}$.)
- using wider jet cone size $\mathbf{R} = 0.8$ to profit from increased agreement displayed by NNLO pQCD predictions.

Following strategy of past HERAPDF analyses ^[1]:

- HERA **DIS** (Deep Inelastic Scattering) data are complemented with aforementioned **CMS** dijet cross sections.
- phase space restricted to $\mathbf{Q}_{\min}^2 = 10 \text{ GeV}$ for HERA data.

[1]: H1 and ZEUS Collaborations, "Combination of measurements of inclusive deep inelastic $e\pm p$ scattering cross sections and QCD analysis of HERA data", *Eur. Phys. J. C* **75** (2015) 580, [doi:10.1140/epjc/s10052-015-3710-4](https://doi.org/10.1140/epjc/s10052-015-3710-4), [arXiv:1506.06042](https://arxiv.org/abs/1506.06042).



QCD analysis – Fit details | PDF-only fits

QCD analysis performed with both **2D** and **3D** cross sections:

- as a function of $\mathbf{m}_{1,2}$ to reach the higher end of the phase space.
(*indications of a smaller impact to subleading color corrections compared to $\langle p_T \rangle_{1,2}$)
- using wider jet cone size $\mathbf{R} = 0.8$ to profit from increased agreement displayed by NNLO pQCD predictions.

Following strategy of past HERAPDF analyses [1]:

- HERA **DIS** (Deep Inelastic Scattering) data are complemented with aforementioned **CMS** dijet cross sections.
- phase space restricted to $\mathbf{Q}_{\min}^2 = 10 \text{ GeV}$ for HERA data.

Fits performed with **xFITTER** interfaced to **FASTNLO**:

- PDF parametrized to \mathbf{x} as
$$xf = A_f x^B f (1-x)^C f (1 + D_f x + E_f x^2)$$
 - Proton structure expressed as
 $f = g(x), u_v(x), d_v(x), \Sigma(x) = 2\bar{U}(x) + \bar{D}(x)$.
 - A, B and C are always included, D and E added based on χ^2 -scan.
- Starting with a **10 parameter** fit prior to χ^2 -scan.
- Both **PDF-only** ($\alpha_S(m_Z) = 0.118$ fixed) and **PDF+ α_S** fits are performed.

[1]: H1 and ZEUS Collaborations, “Combination of measurements of inclusive deep inelastic e±p scattering cross sections and QCD analysis of HERA data”, *Eur. Phys. J. C* **75** (2015) 580, [doi:10.1140/epjc/s10052-015-3710-4](https://doi.org/10.1140/epjc/s10052-015-3710-4), [arXiv:1506.06042](https://arxiv.org/abs/1506.06042).



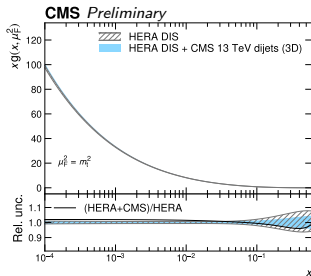
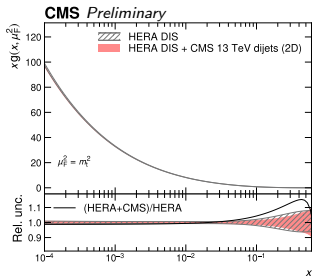
QCD analysis – Final parametrization | PDF-only fits

2D parametrization

$$\begin{aligned}
 xg(x) &= A_g x^{B_g} (1-x)^{C_g} \\
 xu_{\nu}(x) &= A_{u_{\nu}} x^{B_{u_{\nu}}} (1-x)^{C_{u_{\nu}}} (1 + D_{u_{\nu}} x + E_{u_{\nu}} x^2) \\
 xd_{\nu}(x) &= A_{d_{\nu}} x^{B_{d_{\nu}}} (1-x)^{C_{d_{\nu}}} \\
 x\bar{U}(x) &= A_{\bar{U}} x^{B_{\bar{U}}} (1-x)^{C_{\bar{U}}} (1 + D_{\bar{U}} x) \\
 x\bar{D}(x) &= A_{\bar{D}} x^{B_{\bar{D}}} (1-x)^{C_{\bar{D}}} (1 + D_{\bar{D}} x)
 \end{aligned}$$

3D parametrization

$$\begin{aligned}
 xg(x) &= A_g x^{B_g} (1-x)^{C_g} \\
 xu_{\nu}(x) &= A_{u_{\nu}} x^{B_{u_{\nu}}} (1-x)^{C_{u_{\nu}}} (1 + D_{u_{\nu}} x) \\
 xd_{\nu}(x) &= A_{d_{\nu}} x^{B_{d_{\nu}}} (1-x)^{C_{d_{\nu}}} \\
 x\bar{U}(x) &= A_{\bar{U}} x^{B_{\bar{U}}} (1-x)^{C_{\bar{U}}} (1 + D_{\bar{U}} x) \\
 x\bar{D}(x) &= A_{\bar{D}} x^{B_{\bar{D}}} (1-x)^{C_{\bar{D}}} (1 + D_{\bar{D}} x)
 \end{aligned}$$



QCD analysis – Final parametrization | PDF-only fits

2D parametrization

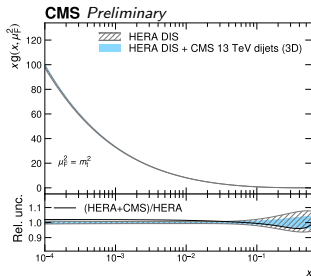
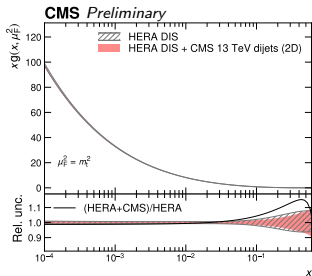
$$\begin{aligned}
 xg(x) &= A_g x^{B_g} (1-x)^{C_g} \\
 xu_{\nu}(x) &= A_{u_{\nu}} x^{B_{u_{\nu}}} (1-x)^{C_{u_{\nu}}} (1 + D_{u_{\nu}} x + E_{u_{\nu}} x^2) \\
 xd_{\nu}(x) &= A_{d_{\nu}} x^{B_{d_{\nu}}} (1-x)^{C_{d_{\nu}}} \\
 x\bar{U}(x) &= A_{\bar{U}} x^{B_{\bar{U}}} (1-x)^{C_{\bar{U}}} (1 + D_{\bar{U}} x) \\
 x\bar{D}(x) &= A_{\bar{D}} x^{B_{\bar{D}}} (1-x)^{C_{\bar{D}}} (1 + D_{\bar{D}} x)
 \end{aligned}$$

3D parametrization

$$\begin{aligned}
 xg(x) &= A_g x^{B_g} (1-x)^{C_g} \\
 xu_{\nu}(x) &= A_{u_{\nu}} x^{B_{u_{\nu}}} (1-x)^{C_{u_{\nu}}} (1 + D_{u_{\nu}} x) \\
 xd_{\nu}(x) &= A_{d_{\nu}} x^{B_{d_{\nu}}} (1-x)^{C_{d_{\nu}}} \\
 x\bar{U}(x) &= A_{\bar{U}} x^{B_{\bar{U}}} (1-x)^{C_{\bar{U}}} (1 + D_{\bar{U}} x) \\
 x\bar{D}(x) &= A_{\bar{D}} x^{B_{\bar{D}}} (1-x)^{C_{\bar{D}}} (1 + D_{\bar{D}} x)
 \end{aligned}$$

Inclusion of CMS data to gluon PDF determination at m_t^2 scale

- Bands illustrate PDF relative fit uncertainty σ_{fit} ,
 - leads to reduction at $x > 10^{-1}$.
- Enhanced central value at $x > 10^{-1}$ for 2D.
- Compatible central value for 3D.

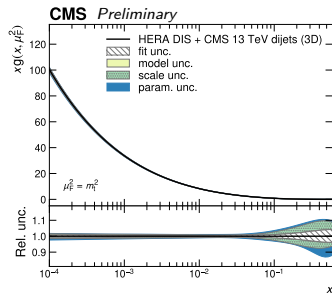
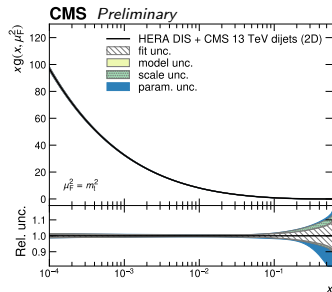


QCD analysis – PDF -only and $PDF+\alpha_s$ fits

Total PDF uncertainty de-composition

- 1 **fit**: Hessian fit uncertainty.
- 2 **scale**: μ_R, μ_F 6-point variation envelope.
- 3 **model**: Sum in quadrature of non-PDF parameter variations (values in [backup](#)).
- 4 **param.**: Envelope of all fits performed with one more E or D parameter than the final parametrization.

$$\sigma_{total} = \sqrt{\sigma_{fit}^2 + \sigma_{scale}^2 + \sigma_{model}^2} + |\sigma_{param.}|$$



Determination of $\alpha_S(m_Z)$ in $PDF+\alpha_S$ fits

- Exact same parametrization is used as in PDF -only fits.

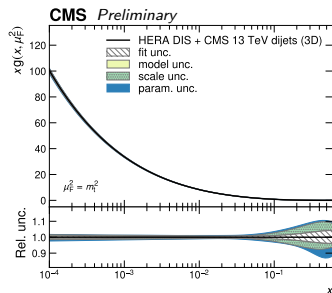
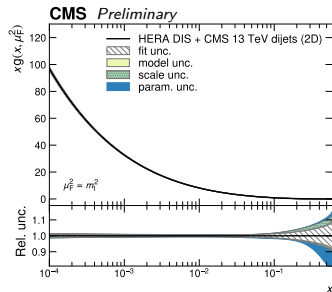
- 2D with $\chi^2/n_{dof} = 1280.47/1093 = 1.172$

$$\alpha_S(m_Z) = 0.1201 \text{ (12)}_{\text{fit}} \text{ (8)}_{\text{scale}} \text{ (8)}_{\text{model}} \text{ (5)}_{\text{param.}} \mid \text{(21)}_{\text{total}}$$

- 3D with $\chi^2/n_{dof} = 1553.27/1166 = 1.332$

$$\alpha_S(m_Z) = 0.1201 \text{ (10)}_{\text{fit}} \text{ (5)}_{\text{scale}} \text{ (8)}_{\text{model}} \text{ (6)}_{\text{param.}} \mid \text{(20)}_{\text{total}}$$

- ~ 1 standard deviation away from current world average value of $\alpha_S(m_Z) = 0.1179 \text{ (9)}_{\text{total}}$.



- Introduction
- Unfolding
- Theory
- QCD analysis
- **Summary**
- Back Up



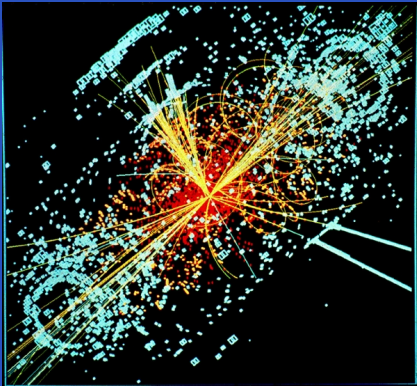
- Multi-differential dijet cross section measurements are presented at 13 TeV:
 - as a function of either $m_{1,2}$ or $\langle p_T \rangle_{1,2}$,
 - investigated under both the $|y|_{max}$ and y^* , y_b rapidity variables,
 - using the standard CMS jet cone sizes of $R = 0.4$ and $R = 0.8$.
- Data are compared to fixed order theory predictions at NNLO accuracy.
 - The latter corrected for NP and EW effects.
 - Agreement is found to be good, mostly below 10%, with $R = 0.8$ jets displaying the better agreement.
- *PDF-only* fits are performed with the inclusion of 2D and 3D cross sections ($m_{1,2}$, $R = 0.8$) to the HERA DIS data.
 - PDFs are further constrained, especially the gluon PDF for $x > 10^{-1}$.
 - Results between 2D and 3D fits compatible taking into account their respective uncertainties.
- *PDF+ α_S* fits are performed for the determination of $\alpha_S(m_Z)$.
 - Nearly identical results between 2D and 3D:
2D: $\alpha_S(m_Z) = 0.1201$ (12)_{fit} (8)_{scale} (8)_{model} (5)_{param.} | (21)_{total}.
3D: $\alpha_S(m_Z) = 0.1201$ (10)_{fit} (5)_{scale} (8)_{model} (6)_{param.} | (20)_{total}.



The research work was supported by the Hellenic Foundation for Research and Innovation (HFRI) under the 3rd Call for HFRI PhD Fellowships (Fellowship Number: 83154).



The End



Thank you for you time!



- Introduction
- Unfolding
- Theory
- QCD analysis
- Summary
- **Back Up**



On Data:

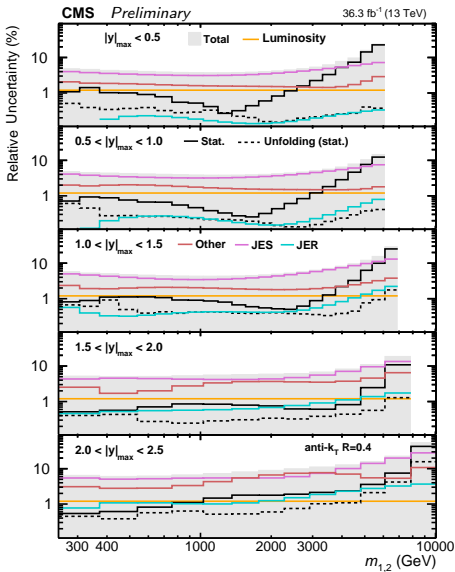
- 1 Raw n-tuple construction + apply basic filters
- 2 Jet Energy Correction
- 3 Normalization
- 4 Prefiring correction

On MC:

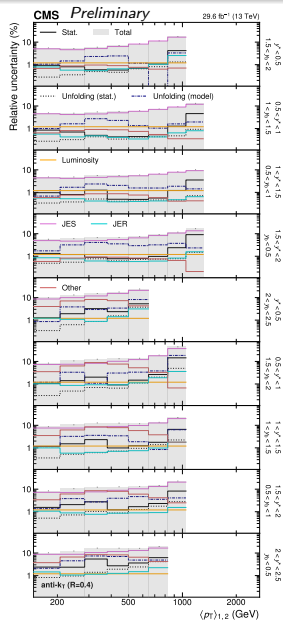
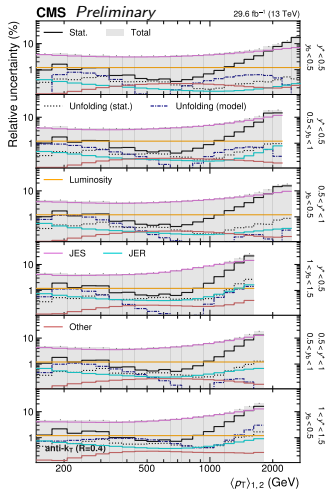
- 1 Raw n-tuple construction + apply basic filters
- 2 Normalization
- 3 Pileup cleaning
- 4 Jet Energy Correction
- 5 Jet Energy Resolution Correction
- 6 Pile Profile Reweighting Correction



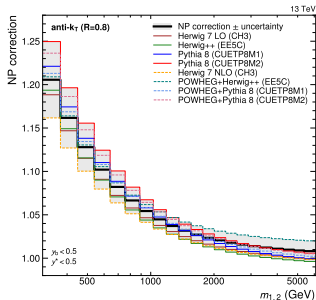
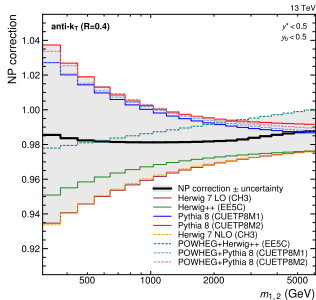
Experimental uncertainties | 2D: $m_{1,2}$, $R = 0.4$



Experimental uncertainties | 3D: $\langle p_T \rangle_{1,2}$, $R = 0.4$



Non-Perturbative (NP) Corrections factors



- Theory \rightarrow at **Parton** Level
- Data \rightarrow at **Particle** Level
- Theory $\otimes C_{NP_s} \rightarrow$ corrected for **NP effects** (e.g., Hadronization and Multiple Parton Interactions)

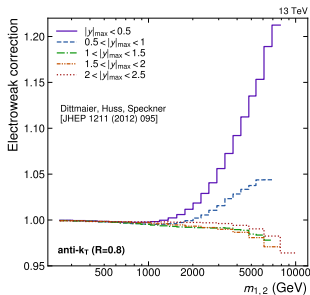
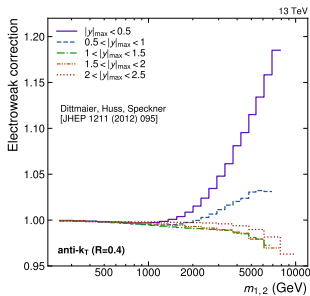
where,

$$C_{NP_s} = \frac{MPI_HAD_on}{MPI_HAD_off} = \frac{\sigma^{PS+HAD+MPI}}{\sigma^{PS}}$$

- C_{NP_s} around unity for $R = 0.4$.
- Larger C_{NP_s} at lower $m_{1,2}$ for $R = 0.8$.



Electroweak (EW) Correction factors



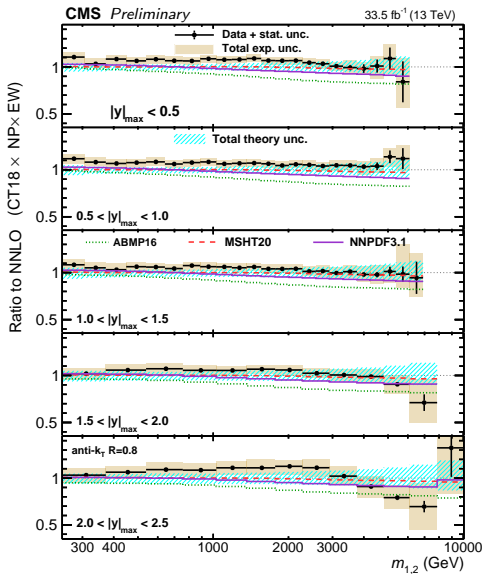
Above 1 TeV electroweak effects become important:

(virtual exchange of soft or collinear W or Z bosons)

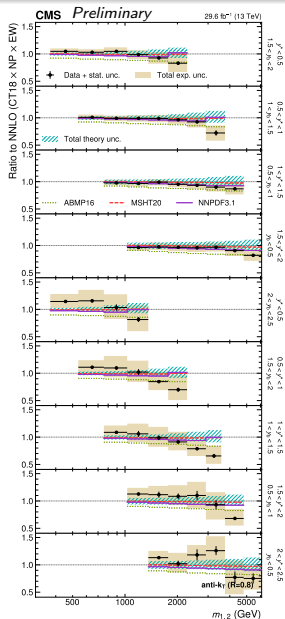
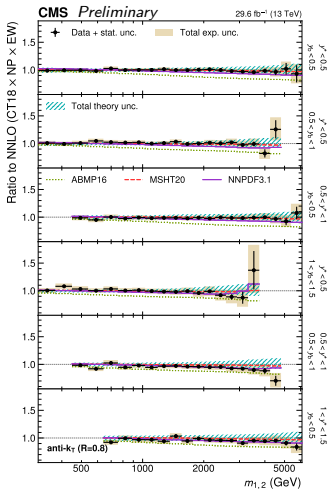
- Theory $\otimes C_{NP_s} \otimes C_{EW}$
- EW factors dominant for large $m_{1,2}$ values and central $|y|_{max}$ regions
- At central $|y|_{max}$ regions up to $\sim 20\%$
- Change in sign for forward $|y|_{max}$ regions



Ratio Data over Theory | 2D: $m_{1,2}$, $R = 0.8$



Ratio Data over Theory | 3D: $m_{1,2}, R = 0.8$



2D partial χ^2 values for *PDF-only* fits

Data set	Partial χ^2 / n_{data}	
	HERA DIS only	HERA DIS + CMS dijets (2D)
CMS dijet 2D		
$ y _{\text{max}} < 0.5$		24 / 22
$0.5 < y _{\text{max}} < 1$		14 / 22
$1 < y _{\text{max}} < 1.5$		22 / 23
$1.5 < y _{\text{max}} < 2$		15 / 12
$2 < y _{\text{max}} < 2.5$		30 / 12
HERA1+2 CCem	52 / 42	50 / 42
HERA1+2 CCep	37 / 39	37 / 39
HERA1+2 NCem	221 / 159	222 / 159
HERA1+2 NCep 460	199 / 177	197 / 177
HERA1+2 NCep 575	186 / 221	186 / 221
HERA1+2 NCep 820	56 / 61	55 / 61
HERA1+2 NCep 920	363 / 317	368 / 317
Total χ^2 / n_{dof}	1161 / 1003	1283 / 1094



3D partial χ^2 values for *PDF-only* fits

Data set	Partial χ^2 / n_{data}	
	HERA DIS only	HERA DIS + CMS dijets (3D)
CMS dijet 3D		
$y_b < 0.5$ $y^* < 0.5$		32 / 21
$y_b < 0.5$ $0.5 < y^* < 1$		23 / 19
$0.5 < y_b < 1$ $y^* < 0.5$		40 / 19
$y_b < 0.5$ $1 < y^* < 1.5$		45 / 17
$0.5 < y_b < 1$ $0.5 < y^* < 1$		18 / 17
$1 < y_b < 1.5$ $y^* < 0.5$		44 / 17
$y_b < 0.5$ $1.5 < y^* < 2$		15 / 7
$0.5 < y_b < 1$ $1 < y^* < 1.5$		7 / 7
$1 < y_b < 1.5$ $0.5 < y^* < 1$		9 / 7
$1.5 < y_b < 2$ $y^* < 0.5$		20 / 6
$y_b < 0.5$ $2 < y^* < 2.5$		19 / 6
$0.5 < y_b < 1$ $1.5 < y^* < 2$		16 / 6
$1 < y_b < 1.5$ $1 < y^* < 1.5$		6 / 6
$1.5 < y_b < 2$ $0.5 < y^* < 1$		1 / 5
$2 < y_b < 2.5$ $y^* < 0.5$		15 / 4
HERA1+2 CCem	52 / 42	48 / 42
HERA1+2 CCep	37 / 39	41 / 39
HERA1+2 NCem	221 / 159	227 / 159
HERA1+2 NCep 460	199 / 177	201 / 177
HERA1+2 NCep 575	186 / 221	187 / 221
HERA1+2 NCep 820	56 / 61	55 / 61
HERA1+2 NCep 920	363 / 317	365 / 317
Total χ^2 / n_{dof}	1168 / 1003	1557 / 1167

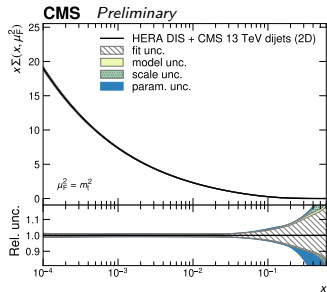
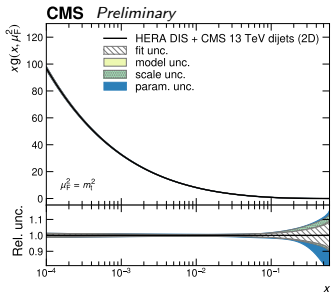
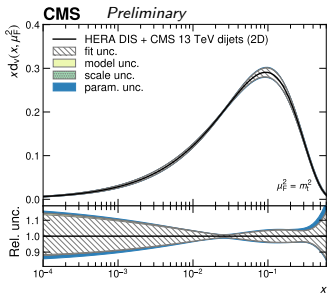
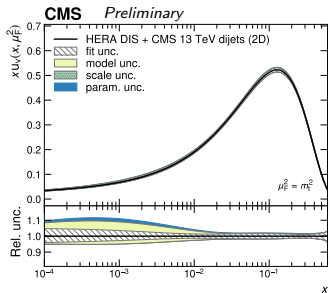


Non-PDF parameter values and variations

- Values with asterisk fail to meet the $\mu_{F,0} < m_c$ s requirement.
 - these values are symmetrized according to the opposite variation value.

Parameter	Nominal value	Variations	
		<i>down</i>	<i>up</i>
Q_{\min}^2 (GeV ²)	10	7.5	12.5
f_s	0.4	0.3	0.5
m_c (GeV)	1.43	1.37*	1.49
m_b (GeV)	4.5	4.25	4.75
$\mu_{E,0}^2$ (GeV ²)	1.9	1.6	2.2*





3D PDF-only fits

